Materials for Renewable and Sustainable Energy
https://doi.org/10.1007/s40243-024-00261-y

ORIGINAL PAPER

Numerical investigation of the effect of an air layer on the melting process of phase change materials

Abbas Fadhil Khalaf[1] · Farhan Lafta Rashid[1] · Mudhar A. Al-Obaidi[2,3] · Arman Ameen[4] · Hayder I. Mohammed[5]

Received: 28 February 2024 / Accepted: 26 April 2024

Abstract

Designing more effective thermal energy storage devices can result from understanding how air layers impact the melting process. The total efficiency of these systems can be improved by optimizing the melting process of the phase change materials (PCMs), which are utilised to store and release thermal energy. The current study utilises an analysis to evaluate how an air layer would affect melting of the PCM. The enthalpy-porosity combination based ANSYS/FLUENT 16 software is specifically used to accomplish this study, considering the paraffin wax (RT42) as the PCM. The study reveal that the presence of an air layer would impact the dissolution process. This result is assured an increase of melting time of PCM by 125% as a result to having an air layer of 5 cm thickness compared to a cell without an air layer. Furthermore, an increase of the layer thickness beyond 5 cm has a progressive effect on the melting time of PCM. One important component that affects the melting process is the existence of an air layer above the cell. Greater heat transfer resistance from thicker air layers prolongs the time needed to finish melting. The efficient heat transmission of PCM is shown to be reduced when there is an air layer above the cell. The melting process gradually slows down as the air layer thickness rises, which reflects the decreased heat transmission. These results highlight how crucial it is to take the environment into account while creating PCM-filled energy storage cells.

Keywords Phase change materials (PCMs) · Layer of air · Melting process · Paraffin wax · Thermal energy storage · Latent heat

✉ Arman Ameen
arman.ameen@hig.se

Abbas Fadhil Khalaf
abbas.fadhil@uokerbala.edu.iq

Farhan Lafta Rashid
farhan.lefta@uokerbala.edu.iq

Mudhar A. Al-Obaidi
dr.mudhar.alaubedy@mtu.edu.iq

Hayder I. Mohammed
hayder.i.moahmmad@garmian.edu.krd

[1] Petroleum Engineering Department, College of Engineering, University of Kerbala, Karbala 56001, Iraq

[2] Technical Institute of Baquba, Middle Technical University, Baquba 32001, Iraq

[3] Technical Instructor Training Institute, Middle Technical University, Baghdad 10074, Iraq

[4] Department of Building Engineering, Energy Systems and Sustainability Science, University of Gävle, 801 76 Gävle, Sweden

[5] Department of Cooling and Air Conditioning Engineering, Imam Ja'afar Al-Sadiq University, Baghdad 10011, Iraq

List of symbols

C	Mushy zone constant,-
C_p	Specific heat capacity, J/kg K
g	Acceleration, m/s^2
h	Sensible enthalpy, J/kg
h_{ref}	Reference sensible enthalpy, J/kg
H	Specific enthalpy, J/kg
ΔH	Latent heat, J/kg
K	Thermal conductivity, W/mK
L_f	Latent heat melting of liquid, J/kg
P	Pressure, Pa
S	Darcy's law damping term, –
t	Time, s
T	Operating temperature, K
T_{ref}	Reference temperature, K
T_l	Liquid temperature, K
T_m	Melting temperature, K
T_s	Solid temperature, K
V	Velocity, m/s
α	Thermal expansion rate, 1/K
β	Liquid fraction, –

Published online: 14 May 2024

ρ Density, kg/m^3
μ Dynamic viscosity, kg/m s

Introduction

The worldwide energy demand has enlarged continuously as a result to the industrial revolution. Total primary energy demand enlarged by 70% between 1991 and 2012, from 91,200 to 155,400 TWh, with an estimation to be risen by 40% in 2040. Roughly 15% of today's energy demand is now met by renewable resources. However, greenhouse gases released in the energy sector must be excluded to prevent an environmental disaster [1, 2]. In this regard, the energy from renewable sources should be stored for further use. Storing the energy by latent heating of the PCM has revealed to be an encouraging choice for energy [3, 4]. PCM has been ascertained as an ideal product of thermal energy storage with providing thermal barriers or insulation property. The melting behavior of paraffin wax, an example of PCMs, was fabricated in shell and tube latent heat thermal storage units (LHSU) with different shapes and orientations [5]. Homogeneous mixing of nanoparticles with high thermal conductivity can advance the thermal conductivity of the liquid [6]. Nanofluids are extensively utilised to improve the heat transfer of different materials. Similarly, an addition of nanoparticles to PCM can be a crucial method to enhance its thermal conductivity [7].

Research on PCMs in tube-shell storage systems, particularly in circular tubes, has been conducted using numerical and experimental approaches. To further discover this area, De Gracia et al. [8] added PCM enclosed in 57 vertical pipes to a residential electrical hot water cylinder. Comparably, Mat et al. [9] used three different ways (heating the interior tube, heating the outside tube, and heating both sides) to quantitatively study the melting process in a triplex-tube heat exchanger for PCM melting. Shabgard et al. [10] took a different tack when they used a thermal network model to examine the advantages of adding several heat pipes between PCM and a heat transfer fluid. The inclusion of heat pipes was shown to enhance thermal efficiency.

Tao and Carey [11] experimentally examined the influences on the thermal storage performance of a shell-and-tube latent heat storage unit by examining the thermos-physical properties of PCM. The heat transfer fluid (HTF) in the examination was run via a circular tube. To enhance the rate and quality of the entire storage process, the research made clear how significant it is to choose PCM with high density, specific heat, melting enthalpy, and thermal conductivity besides having a low melting temperature. Using a different approach, Allouche et al. [12] developed a Computational Fluid Dynamics (CFD) model to mimic the process of PCM energy storage in a 100-L cylindrical tank positioned horizontally. A horizontal tube bundle contained water that was utilised to charge the cold storage unit. It was revealed that the simulated heat transfer rate and experimentation approved fairly well. To discourse the effects of gas injection tube diameter, heat environment, and gas injection time on nucleation and crystallization features, Hou et al. [13] offered a novel nucleation method including gas injection agitation and seeding. Encouraging results from the experimental research exhibited that, under ideal conditions, the solidification enthalpy can reach 203.1 J/g, which is corresponding to 85% of the melting enthalpy. After 100 heating and cooling cycles, the material also disclosed exceptional thermal cycle stability. The influence of Multi-Walled Carbon Nanotube (MWCNT) nanoparticle additions on nucleation was also examined in this research.

El Hasadi [14] tested the formation of the solid–liquid interface, the distribution profiles of nanoparticles, and thermal convection when melting colloidal suspensions of nanostructured PCM inside a rectangular cavity. The single-domain enthalpy-porosity model for phase change was combined with the one-fluid-mixture technique in the numerical model. Particularly, under melting conditions, the study perceived alterations in the morphology of the solid–liquid interface. Heat pipes with U-shaped designs were considered by Ebrahimi et al. [15] to increase latent heat storage. Thirteen models were inspected, using water as the HTF and RT-35 as the PCM. By placing the heat pipe around the single pipe heat storage system, the melting time was established to be meaningfully reduced, up to 91%. The influence of the tube plant angle on melting time was also highlighted by the study. Yan et al. [16] achieved out tests to mimic the operational conditions of a residential hot water system and proposed a heat transfer augmentation method utilising ultrasonic. With an improved natural convection of PCM throughout the charging process and an augmented average heat transfer coefficient, ultrasound was found to radically reduce the latent heat storage (LHS) unit's charging time.

Park et al. [17] deployed an enthalpy-porosity model to mimic the phase change process in a multi-tube shell-and-tube latent heat thermal energy storage system. The intention was to discover the influence of the number and configuration of tubes on PCM melting performance. Eight various tube configurations were evaluated in the study to evaluate how they affected the melting properties, energy density, liquid fraction, temperature distributions, rates of heat transmission, and melting time. A pore-scale numerical model for simulating PCM melting in a PCM-metal foam composite energy storage system was presented by Parida et al. [18]. The outcomes exhibited that greater pore sizes and higher porosity increase the effect of convection. A comprehensive investigation was accomplished by Zeng et al. [19] using both experimental and mathematical approaches to assess the consequence of inclination angle on the solid–liquid

PCM melting processes. The melting of paraffin under mechanical vibration was the key emphasis of the researchers, who distinguished prominent effects on the melting interface, melting rate, and heat transport.

The melting process of PCM integrated with nanoparticles and metal foams in a large-scale shell-and-tube based latent thermal energy storage unit was mathematically developed by Chibani et al. [20]. With an eminent decrease in melting time, the research established the upgraded performance of MF-PCM systems over nano- and pure-PCM. The order of the satisfactory effect of MFs was Cu > Al > Ni > Ti, which agrees to thermal conductivity. A reduced melting time was obtained by increasing the porosity of the metal foam. In order to shorten charging times and boost energy, Jaberi Kosroshahi and Hossainpour [21] proposed an innovative concurrent use of longitudinal fins and storage rotation approaches. The outcomes specified that inserting the fin on the lower half of the fixed storage would quicken the melting process. It was concluded that concurrent use of storage rotation and embedded longitudinal full-scale fins can attain a 72% discount in complete melting time and a 115% upsurge in total cumulative stored energy, that is associated to the optimised case. The optimised scenario has four fins with an angle difference of 90° and two vertical stop steps with an angle of 180°.

Li et al. [22] utilised advanced fins that mix parallelogram and rectangular fins to appraise the melting of PCM. Researchers analysed, in two-dimensional and using a numerical solution, the melting behavior of several fin models with variable angles under constant flux circumstances in a rectangular cavity. The left wall of the storage was exposed to a heat flux of 2500 W/m^2. The main aim of this investigation was to present fins with innovative models, that are a mix of rectangular and parallelogram fins, to improve the melting performance of PCM. The outcomes showed that amongst variable geometries studied by fin, suggested geometry of model E was nominated among the other models. Altering the fin model has condensed the melting time, that directed to a greater energy charging rate. Furthermore, by appraising various melting angles, the minimum and maximum melting times happened at 60° and 0°, respectively.

The precise examination of the previous studies published in the open literature would assure the absence of a specific study to critically evaluate the influence of having an air layer on the melting time of PCM. Thus, the current study comes to resolve this challenge by considering a cell of different dimensions to elucidate the effect of the presence of a layer of air on the process of melting PCM. This in turn would enable to perceive the importance of having air layer on PCMs that commonly used as energy storage systems. To systematically conduct this study, four different cases are demonstrated: with and without the presence of air layer, while considering different thickness of air layer of 5 cm, 10 cm, and 15 cm with a thorough analysis using ANSYS/FLUENT 16 software.

Numerical procedure

Physics models

This investigation involves analyzing a cell with diverse dimensions, featuring a base measuring 15 cm, a top dimension of 22.5 cm, and a height of 15 cm. The air layer, positioned above the cell, has a base dimension of 22.5 cm and a top dimension of 25 cm. The height of the air layer extends uniformly in all directions at intervals of 5, 10, and 15 cm, as illustrated in Fig. 1. The physical model, including the

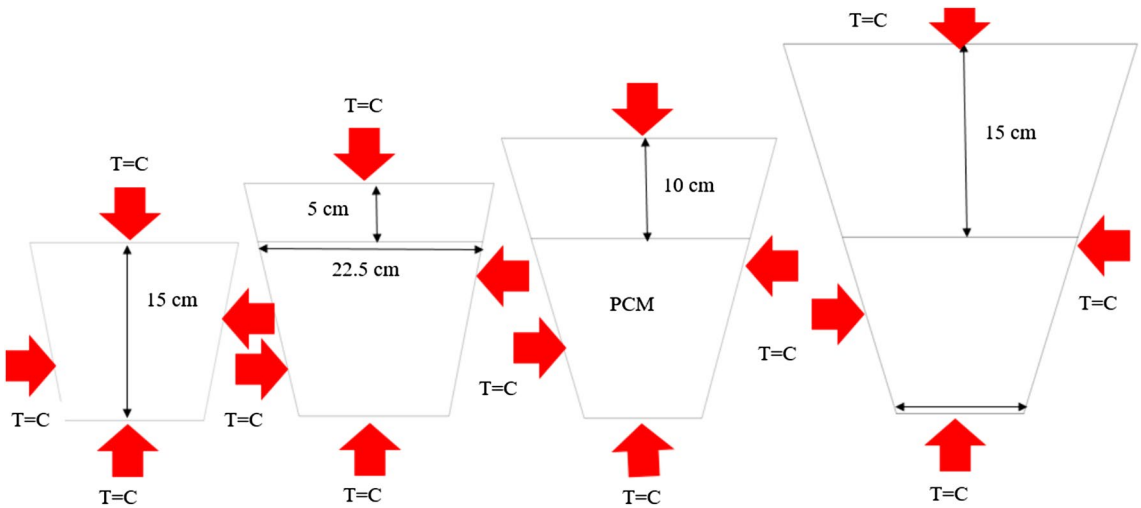

Fig. 1 Formation of physical model

representation of the air layer and PCM, aims to reflect real-world conditions by considering material homogeneity and isotropy in the numerical simulations. On top of this, the impact of the air layer's thickness on melting time and heat transfer resistance of the PCM is quantified using the enthalpy-porosity method within the ANSYS/FLUENT 16 software, which considers the specific heat capacity, density, and latent heat of the PCM. The presence of the air layer introduces additional thermal resistance, affecting the heat transfer dynamics and subsequently influencing the melting process duration. However, there are limitations in the model's assumptions regarding these properties, as real materials may exhibit non-uniformities or anisotropic behavior that are not fully captured in the simulation. Additionally, the model's representation of the air layer and PCM interface may simplify the actual complexities of heat transfer at this boundary.

The thermal features of the PCM (paraffin wax RT42), are incorporated into the numerical model through parameters like thermal conductivity, specific heat capacity, and latent heat. These properties play a critical role in determining the heat transfer rates, temperature gradients, and overall melting behavior of the PCM in response to external factors like the air layer thickness.

Computational procedure

Numerical analysis enables the prediction of specific information of the melting processes that take place in the half-cylindrical cell. The flow was found to be 2D, laminar, incompressible, and unstable. To denote melting processes, it is presumed that the liquid and solid phases are homogeneous, isotropic, and preserve thermal equilibrium at the interface. The enthalpy-porosity method was used to model the PCM. Several assumptions are made in this model, including the conservation of energy, mass, and momentum during phase change, in addition to the presumption of local thermal equilibrium within the PCM. By employing the enthalpy-porosity approach, the model accounted for the complex heat transfer phenomena associated with phase change processes, including those occurring in the presence of an air layer. The melting processes of PCMs are deliberated inherently problematic as a result to their non-linearity, temporal conduct, and a static movement of the solid–liquid boundary. The repeatability of numerical results across different simulation runs is assessed by performing multiple simulations under consistent conditions and comparing the outcomes for consistency.

Natural convection within the PCM is accounted for in the model by considering fluid flow and heat transfer driven by density gradients. The varying thickness of the air layer above the PCM affects the natural convection patterns and heat transfer rates, influencing the duration and efficiency of the melting process. The model addresses these complexities to provide a comprehensive analysis of the PCM's behavior.

The simultaneous continuity, momentum, and energy governing partial differential modelling equations, which are represented by Eqs. (1–3), respectively, address the melting processes of PCMs [23]:

$$\frac{\partial \rho}{\partial t} + \nabla.(\rho V) = 0 \tag{1}$$

$$\frac{\partial(\rho v)}{\partial \mathrm{t}} + \nabla.(\rho V) = -\nabla P + \mu \nabla^2 V + \rho g + S \tag{2}$$

$$\frac{\partial}{\partial t}(\rho H) + \nabla.(\rho V H) = \nabla.(K \nabla T) \tag{3}$$

ρ is density, g is the acceleration due to gravity, t is time, V is velocity, P is the pressure, μ is dynamic viscosity, H is specific enthalpy, S is the source term, and K is the thermal conductivity. In this regard, it should be noted that the fundamental heat transfer equations, including Fourier's law of conduction and Newton's law of cooling for convection in Eqs. (2, 3), are useful for capturing the complex interactions influencing the melting process.

The specific enthalpy (H) is depicted in Eq. (4).

$$H = h + \Delta H \tag{4}$$

$$h = h_{ref} + \int_{T_{ref}}^{T} C_p dT \tag{5}$$

$$\nabla H = \beta L_f \tag{6}$$

h, h_{ref} and ΔH are the sensible enthalpy, reference sensible enthalpy and the latent heat, respectively. C_p and ∇H are the specific heat capacity and the vector differential operator which denotes the standard derivative of the specific enthalpy, respectively. L_f is the latent heat melting of liquid. The meaning of the latent heat ability diverges between one (for a liquid) and zero (for a solid). The liquid fraction (β) can be described as represented in Eq. (7), with the latent heat ability ranges between one for a liquid to zero for a solid [24–26]:

$$\beta = \begin{Bmatrix} 0 \;\; solidus \;\; if T < T_s \\ 1 \;\; liquidus \;\; if T > T_l \\ \frac{T - T_s}{T_l - T_s} \;\; if \;\; T_s \le T \le T_l \end{Bmatrix} \tag{7}$$

T, T_{ref}, T_s and T_l are operating temperature, reference temperature, solid temperature and liquid temperature, respectively. The source term S in the momentum formula is the Darcy's law damping term that is added to

the momentum formula as a result to the effect of phase change on the convection. S is defined by Mohammed [27]:

$$S = \frac{C(1-\beta)^2}{\beta^3} V \tag{8}$$

C is a mushy zone constant, which mirrors the morphology of the melting forepart. This fixed is a big number, usually (10^4–10^7). In the current research C is presumed constant and is considered to be 10^5 [28].

Boundary conditions

The cell under investigation is insulated on three sides, with heat passing through the side left exposed. A temperature of 77 °C is applied to the wall. The PCM used is RT42 paraffin wax, with its thermal properties provided in Table 1 as well as the data for the air layer. Numerical modeling predicts varying PCM melting behavior compared to paraffin wax. Higher thermal conductivity is likely to result in faster melting, while lower conductivity may lead to slower melting. By adjusting the thermal properties of the PCM in the mathematical model, it allows exploration of these variations and the air layer's impact on thermal performance.

Assumptions

A number of assumptions are deliberated in this investigation to appraise the melting processes inside a rectangular cell [30, 31]:

- 2-D model of melting process is employed,
- fixed thermal features of the PCM in both the liquid and solid phases at the outset,
- The flow is unsteady, laminar, and incompressible,
- The viscous dissipation term is insignificant,
- The influences of volume change related to the solid–liquid phase change are disregarded,
- There is no heat loss or gain from the environment.

Table 1 Thermal properties of the Paraffin (RT42) [29] and air

Properties	RT42	Air
Density,ρ	760 (kg/m^3)	1.1614 (kg/m^3)
Specific heat capacity, C_p	2000 (J/kgK)	1 005 (J/kgK)
Dynamic viscosity, μ	0.02351 (kg/ms)	1.84×10^{-5} (kg/ms)
Thermal conductivity, k	0.2 (W/mK)	0.0261 (W/mK)
Thermal expansion rate, α	0.0005 (1/K)	3.38×10^{-3} (1/K)
Latent heat, L	165,000 (J/kg)	–
Melting temperature, T_m	311.15–315.15 (K)	–

Figure 2 shows the mesh distribution for the model being studied.

Grid independent test

Grid convergence is employed to assess result improvement through the successive reduction of grid sizes in computations [32]. The expectation is that the calculated values should approach the actual solution as the mesh becomes finer. The conventional CFD technique for grid-independence analysis begins with a coarse mesh and regularly upgrades it until the observed changes in results are smaller than a pre-defined satisfactory error. In this study, various mesh sizes (22,500, 28,900, 39,700 and 44,400 grids) were systematically investigated to ensure the independence of the solution from the chosen grid size. The choice of non-proportional grid sizes, such as 22,500, 28,900, 39,700, and 44,400, is based on specific computational requirements and previous experience indicating these sizes as relevant for achieving convergence. While avoiding powers of 2 for grid sizes is a common practice, the selected sequence has been determined based on computational efficiency or accuracy considerations specific to the study's numerical simulations. An acceptable and convenient error value for grid convergence analysis typically ranges from 1 to 5%, depending on the complexity of the simulation and the desired level of accuracy. In this context, an acceptable error of around 3% is considered reasonable for grid convergence analysis in CFD simulations, striking a balance between accuracy and computational efficiency.

The time deviation of volumetric melt fraction for different grid numbers is depicted in Fig. 3. It is evident from Fig. 3 that the deviation in melting time becomes negligible beyond the 44,400-grid meshing system. Consequently, this grid size is deemed sufficient for the current numerical investigation.

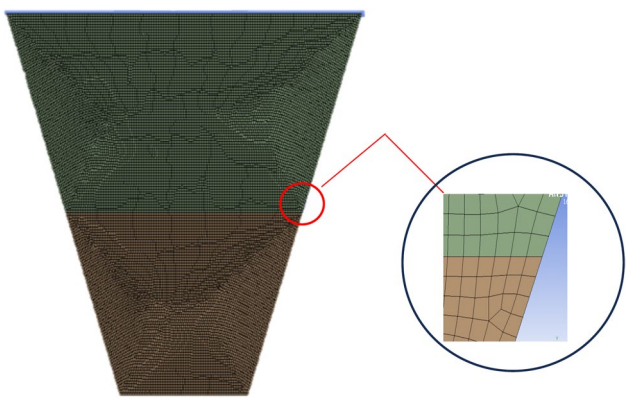

Fig. 2 Formation of the mesh model

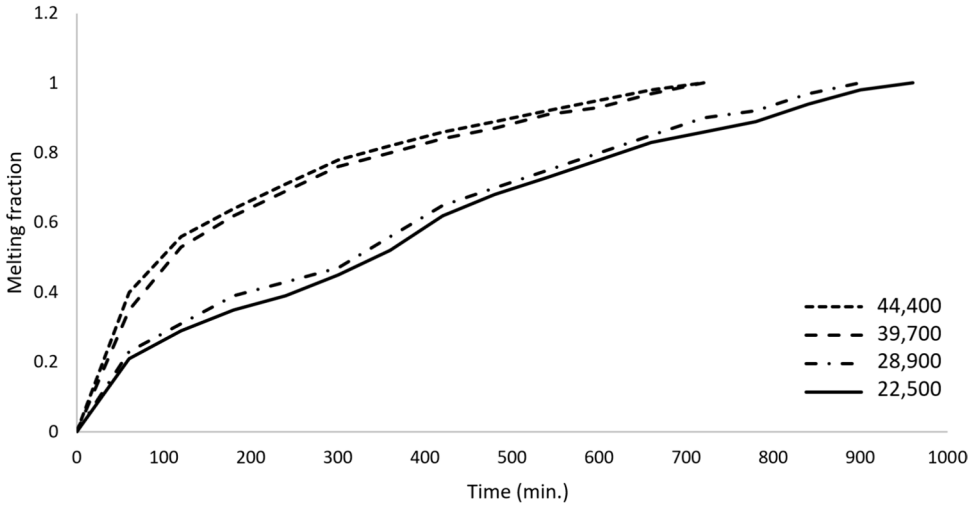

Fig. 3 Melting fraction against operational time of various grid numbers

Validation

This section focuses on interpreting the alignment of numerical results from ANSYS/FLUENT 16 simulations with experimental data or theoretical predictions for the melting process of PCMs. In this regard, a comparison was made between the simulated findings and available experimental data. Specifically, the current work was validated by examining the phase transition progress of RT35 in a double-pipe system through an experimental study conducted by Longeon et al. [33]. This comparison involves analyzing the key parameter of PCM temperature to assess the agreement between the simulation outcomes and the expected behavior based on experimental or theoretical insights. When water was passed through the internal tube, the heat exchanger was positioned vertically, and the PCM was found in the annulus. In terms of the type of thermal management and the PCM and HTF used, the experiment conducted by Longeon et al. [33] and the recent research are extremely equivalent. The mean PCM temperature during melting for the current work and Longeon et al. [33] is shown in Fig. 4. The precision and dependability of the most recent research are shown by the strong agreement between the findings of the current study and the earlier research. The results from both experiments are consistent, indicating the strength and efficacy of the numerical simulations used in this investigation. Furthermore, the present study's results nearly match the experimental result, demonstrating the correctness of the code employed. The strong correlation observed between the experimental results and numerical simulations enhances the reliability of the numerical model employed in this study.

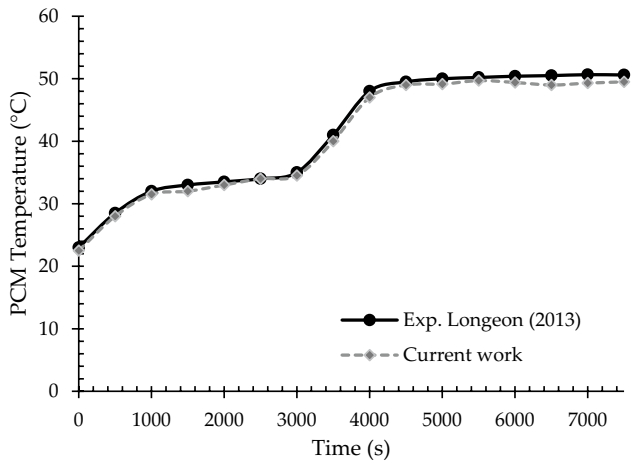

Fig. 4 Melting time of the current study and Longeon et al. [33] in the same conditions

Results and discussion

In the present study, a cell without a layer of air on top is studied to clarify the dissolution process and its effect on the time necessitates to achieve the process. Then, the cell is studied in the presence of an air layer at the top of the cell with different thicknesses, and its effect on the melting process is clarified.

Case one (the cell without layer of air)

In this section, the examination of the cell is conducted without the presence of an air layer. As illustrated in Fig. 5, the initiation of the melting process is influenced by the conduction load along the wall. Subsequently, the melting process transitions to rely on the natural load, becoming

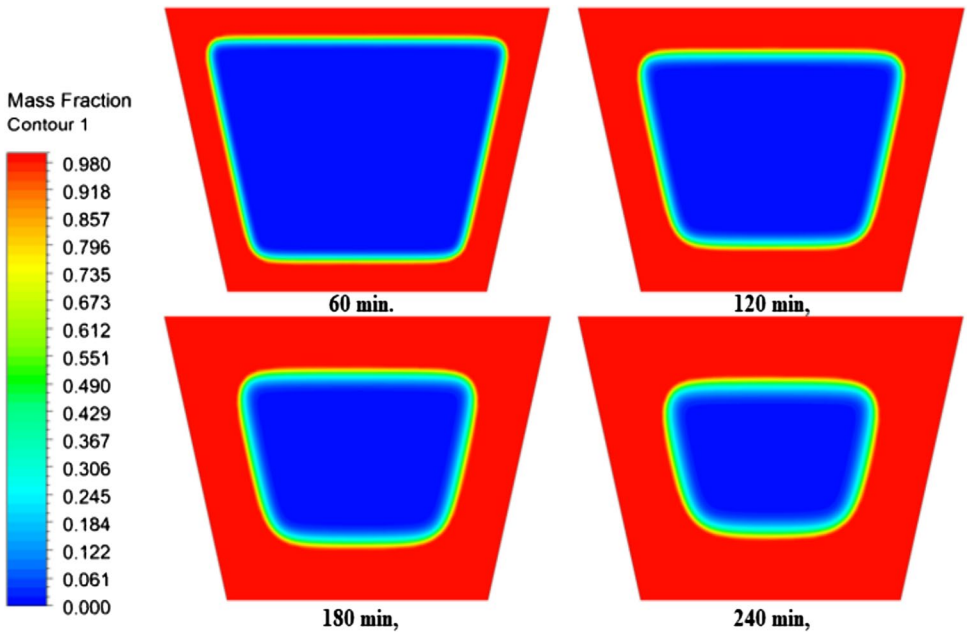

Fig. 5 Anticipated evolution of the melting process without the existence of air layer

more pronounced as the phase-changing materials distance themselves from the wall. Notably, the deceleration of the melting process is apparent with increasing distance from the wall, attributed to the impedance introduced by natural convection. Figure 6 presents the heat transfer to the PCM based on the temperature distribution scheme. Initially, the heat transfer is accelerated due to the dependency on the conduction load. However, as the distance from the wall increases, it decelerates owing to the influence of natural convection.

Case two (with layer of air 5 cm)

In this investigation, the cell is examined under the influence of a 5 cm-wide air layer positioned atop it, as portrayed in Fig. 7. The commencement of the melting process is initiated by the conduction load along the wall. Subsequently, the progression of the melting process be dependent on the natural load, becoming more apparent as the PCM moves away from the wall. The observed deceleration in the melting process away from the wall is attributed to the dependence on natural convection for heat transfer. Notably, the presence of an air layer above the

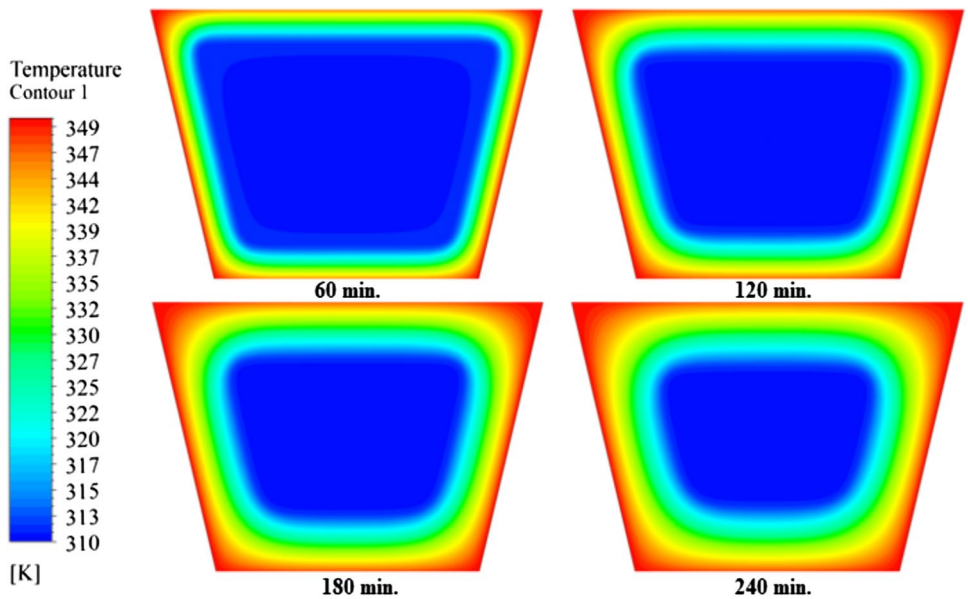

Fig. 6 Temperature distributions without the presence of air layer

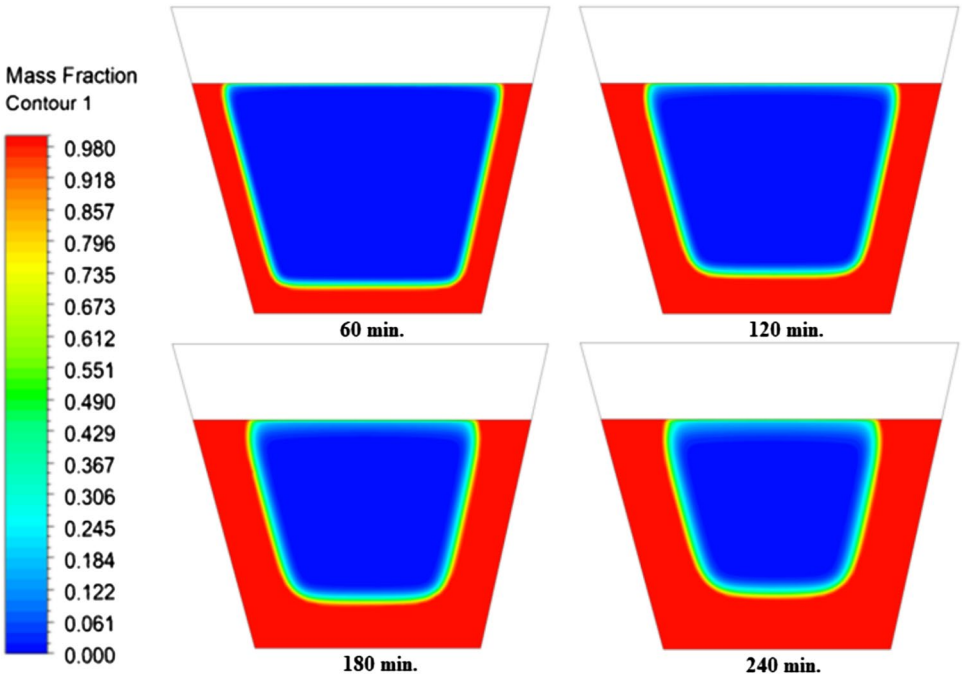

Fig. 7 Anticipated evolution of the melting process with layer of air (5 cm)

cell introduces a discernible influence on the heat transfer dynamics. Illustrated in Fig. 8, the heat transfer into the PCM exhibits an accelerated phase initially, driven by the conduction load. However, with growing distance from the wall, the heat transfer rate diminishes, correlating with the influence of the natural load. Furthermore, it is obvious that the presence of the air layer compromises the PCM's heat transfer capabilities. The progressive effect on melting time with increasing air layer thickness beyond 5 cm eventually plateaus when the thickness reaches a point where the air layer's thermal resistance no longer significantly affects heat transfer dynamics. This plateau can be theoretically explained by the diminishing returns of additional thermal resistance beyond a certain thickness, where the air layer's impact on heat transfer becomes less pronounced due to saturation of thermal resistance effects.

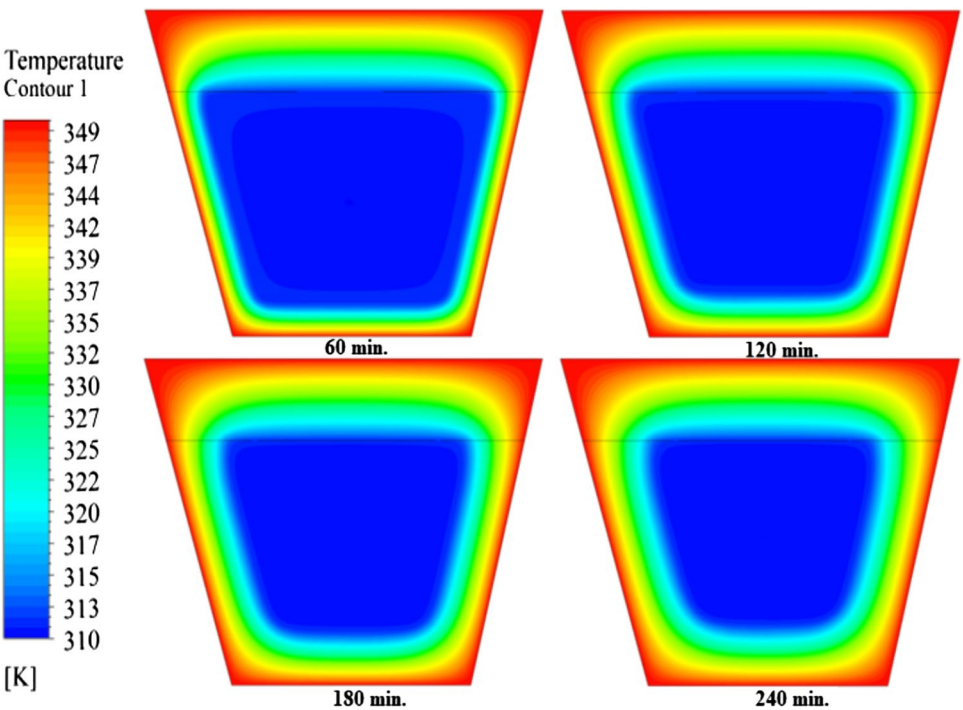

Fig. 8 Temperature distributions with layer of air (5 cm)

Case three (with layer of air 10 cm)

In this investigation, the examination of the cell involves the presence of a 10 cm-wide air layer above it. As illustrated in Fig. 9, the commencement of the melting process is instigated by a conduction stress propagating along the wall. Subsequently, the melting process is significantly influenced by natural convection as the PCM moves away from the wall. The observed deceleration in the melting process, as the distance from the wall increases, is directly attributable to the dependence on natural convection for heat transfer. The presence of the air layer above the cell introduces a distinctive impact on the heat transfer dynamics, which is illustrated in Fig. 10. Initially propelled by the conduction load, the heat transmission to the PCM displays an accelerated phase. Nevertheless, as the distance from the wall upsurges, the heat transfer rate lessens, aligning with the influence of the natural load. In addition, it is notable that the existence of the air layer leads to a drop in heat transport within the PCM. This statement underscores the significant influence

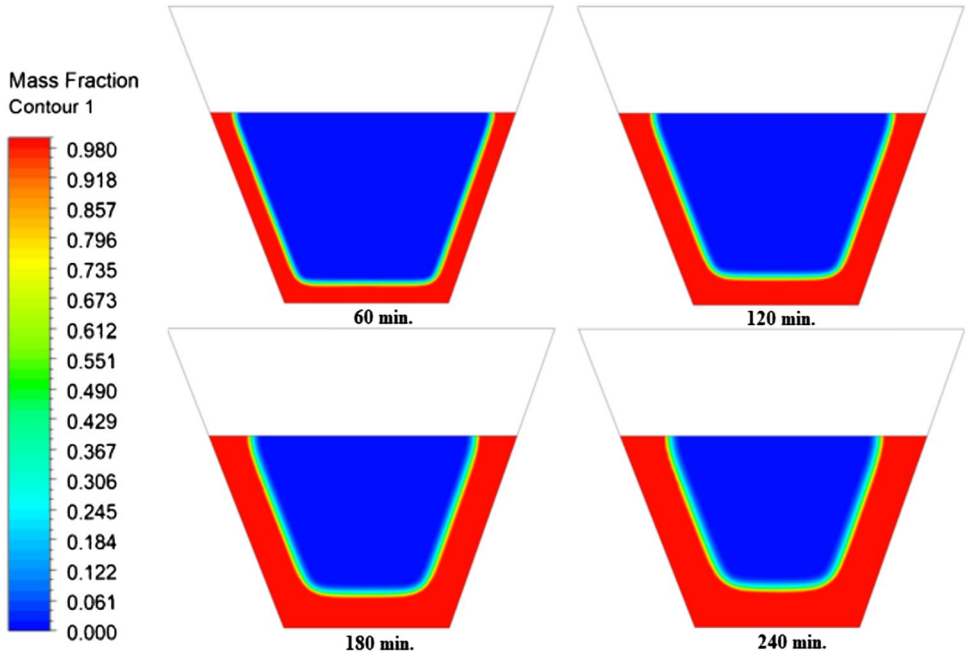

Fig. 9 Anticipated evolution of the melting process with layer of air (10 cm)

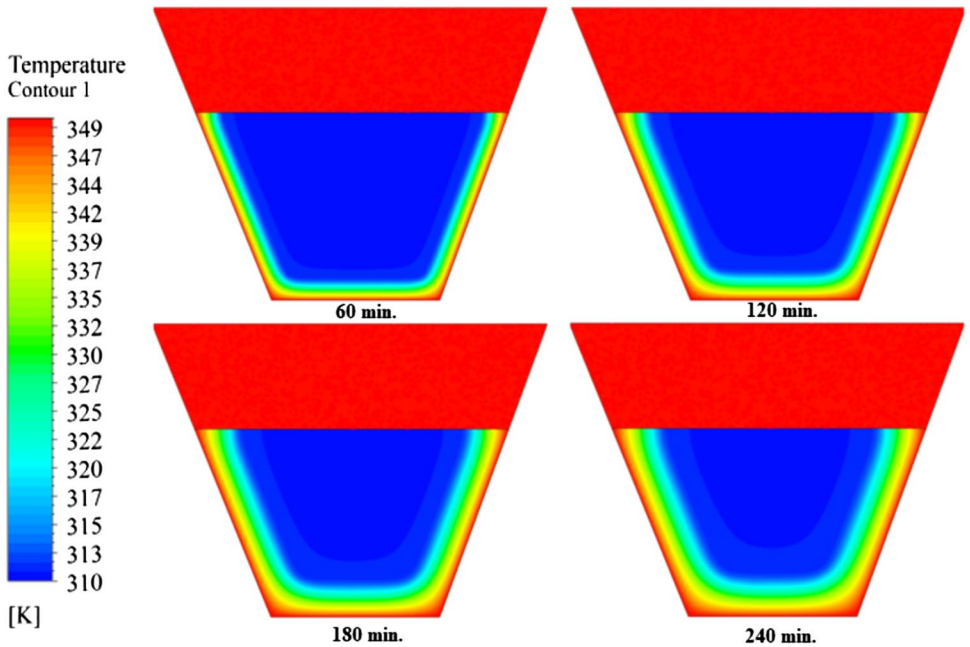

Fig. 10 Temperature distributions with layer of air (10 cm)

of the air layer's thickness on heat transfer, consequently influencing the duration required for the melting process to reach completion. The intricacies of these phenomena are imbedded in the essential principles of heat transfer, where conduction and natural convection dynamics interact with the attendance of the air layer, ensuing the observed variations in the melting process.

Natural convection has a noteworthy role in heat transfer as the PCM moves away from the heat source, with the air layer manipulating convective heat transfer within the PCM by presenting additional thermal resistance. Thicker air layers impede natural convection, leading to reduced heat transfer rates and prolonged melting times. This has implications for melting efficiency as it underscores the need to consider the impact of air layers on convective heat transfer when designing PCM-filled energy storage cells.

Case four (with layer of air 15 cm)

The investigation in this case centers on a cell that has an air layer 15 cm wide above it. Based on the results of in sections "Case two (with layer of air 5 cm)" and "Case three (with layer of air 10 cm)", the following reasonable hypothesis may be made: a rise in the air layer thickness ought to cause a drop in heat transmission, which in turn should prolong the time it takes for the melting process to be completed. This anticipation is consistent with known heat transfer principles, according to which it is expected that thicker air layers will prevent heat from being transferred. As Fig. 11 shows, a conduction stress along the wall drives the melting process to commence. Then, when the Phase Change Material (PCM) moves away from the wall, natural convection becomes more significant and influences how the melting process proceeds. The melting process exhibits a noticeable slowdown with growing distance from the wall, which can be attributed to its dependence on natural convection for heat transfer. A graphic illustration of the changing heat transfer into the PCM is presented in Fig. 12, where the conduction load is in charge for the first stage of increased efficiency. On the other hand, the heat transmission rate declines with growing distance from the wall due to the effect of natural load. The perceived phenomena can be understood in terms of fluid dynamics and heat transfer theories, where the melting process dynamics are formed by the collaboration between conduction, natural convection, and air layer thickness. This thorough analysis highlights the complex interaction between air layer thickness and heat transfer dynamics, enlightening the essential mechanisms that control the PCM melting process's temporal features when the air layer's dimensions fluctuate.

The optimum air layer thickness for the highest efficiency of PCM-based thermal energy storage systems is unyielding based on a balance between thermal resistance and heat transfer efficiency. By allowing for the trade-off between increased thermal resistance and the necessity for effectual heat transfer, an optimal air layer thickness can be recognized that minimizes heat loss, decreases melting time, and improves overall system performance. This statement is normally achieved through numerical simulations and sensitivity analyses to optimise the design of PCM-filled energy storage cells for maximum efficacy.

Comparison of the four studied cases

The comparison of the cases under investigation reveals the observable impact of an air layer above the cell, which significantly affects the complex dynamics of the melting

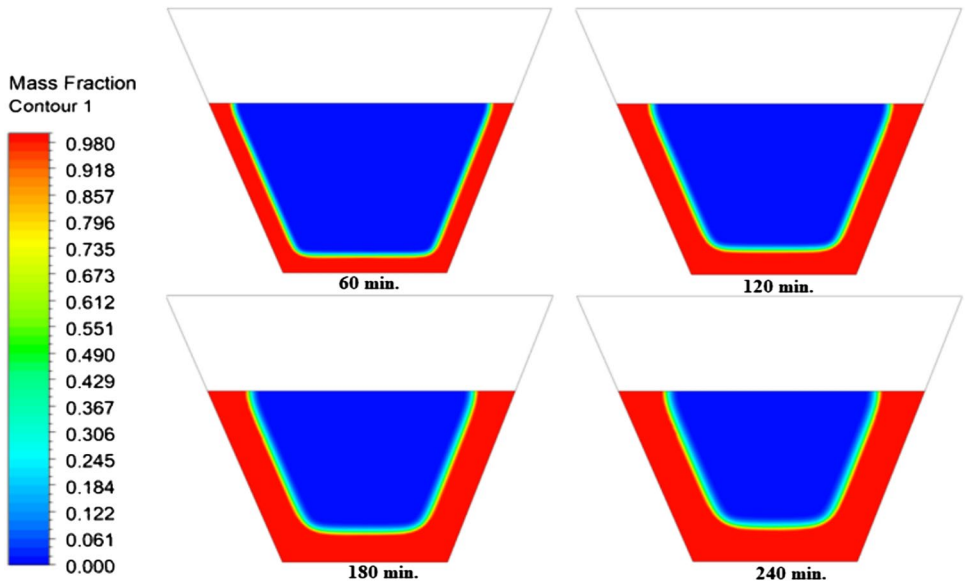

Fig. 11 Anticipated evolution of the melting process with layer of air (15 cm)

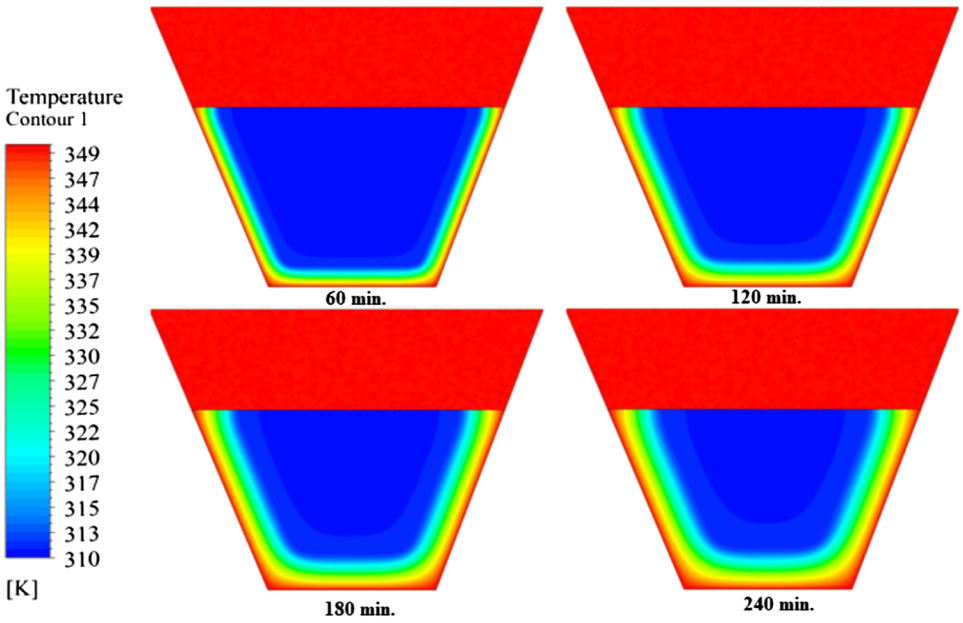

Fig. 12 Temperature distributions with layer of air (15 cm)

process. First and foremost, the air layer modifies the heat transfer mechanism significantly, which in turn determines how long the melting process takes to complete. This transformation is most prominently seen during the dissolving phase, where the presence of an air layer above the cell (seen in Fig. 13) significantly alters the melting process's spatial dynamics. Three sides of a normalized melting process are shown in Fig. 13, however the aspect that coincides with the air layer shows a significantly slower pace because of the air layer's inhibiting effect. Figure 14 illustrates the impact of the air layer in detail by showing how heat moves across the specified area. It is noteworthy that the air layer's thickness has an impact up to a certain point, after which it becomes insignificant. This observation is consistent with the expected dynamics of heat transfer behavior with respect to different air layer thicknesses. Figure 15 shows a visual representation of the air layer's subsequent impact on heat conduction inside the PCM and, in turn, the timing of the melting process. The direct relationship between air layer dimensions and temporal efficiency is highlighted by the fact that an increase in air layer thickness has a proportionate influence on the amount of time needed to complete melting. When a cell has a 5 cm air layer, the amount of time required for melting increases by 125%; when a cell has a 10 cm air layer, the increase is 136%; and when a cell has a 15 cm air layer, the increase is 145%. The localized temperature profile shown in Fig. 16 near the middle of the upper surface of the cell helps to clarify the thermal consequences of an air layer. Most notably, the addition of air causes a significant drop in temperature; this effect becomes less significant as the air layer gets thicker. This detailed study offers a sophisticated comprehension of the complex interactions between

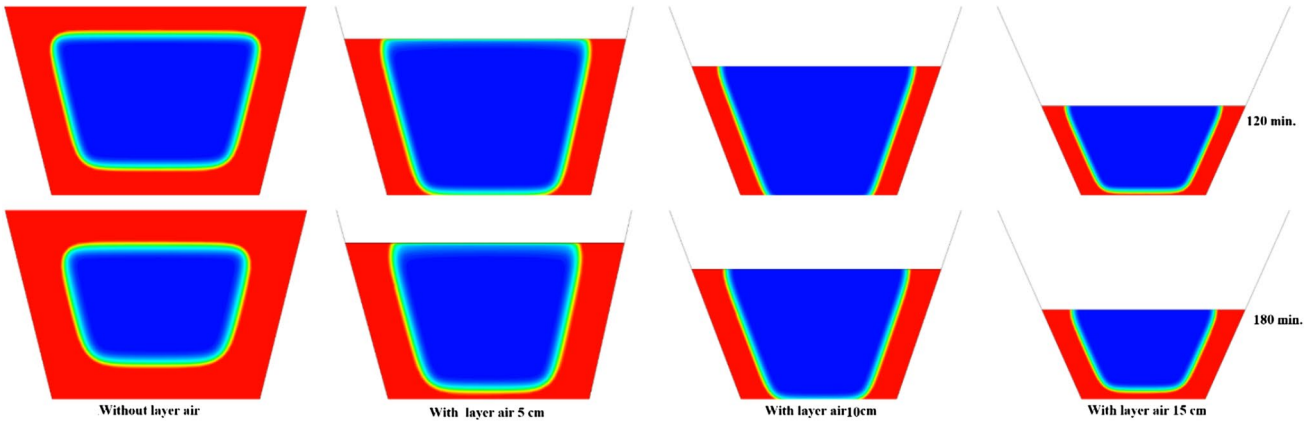

Fig. 13 Comparison of the melting process between the studied cases

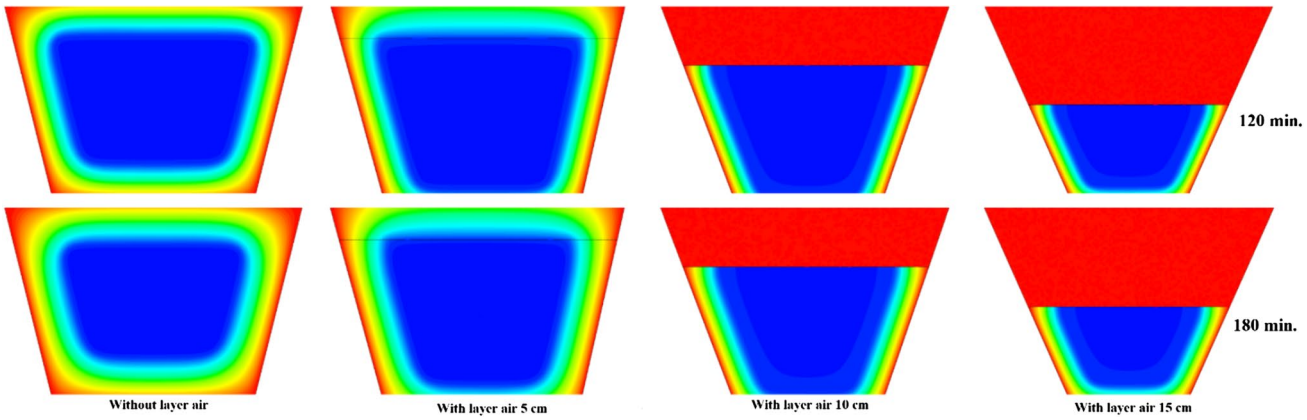

Fig. 14 Comparison of the temperature between the studied cases

Fig. 15 Variation of melt fraction over time

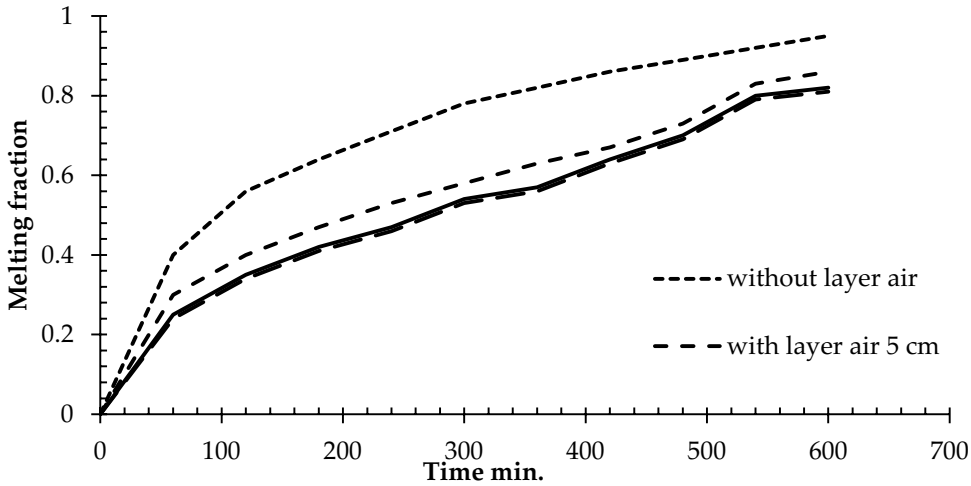

Fig. 16 Distinction of temperature in contradiction to the time of diverse angles of inclination

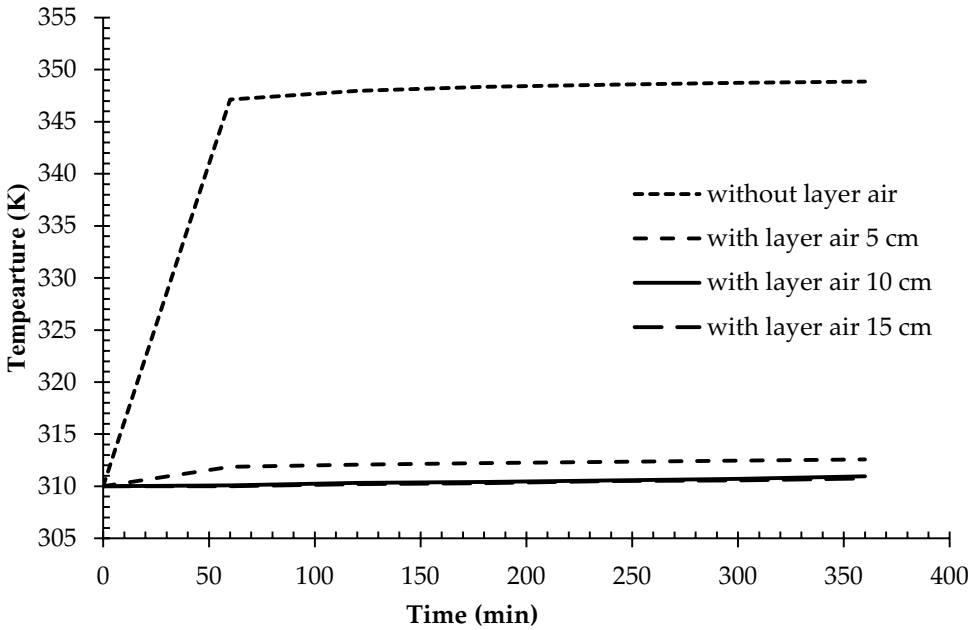

properties of the air layer and their ensuing effects on melting efficiency and heat transmission dynamics.

Generally, the numerical results consider the geometry of the PCM container by considering factors such as shape, size, and orientation that can affect heat transfer and melting efficiency. Geometrical configurations that minimize the negative impact of the air layer may involve optimizing the container design to reduce thermal resistance between the PCM and the air layer, enhancing heat transfer efficiency, and promoting more uniform temperature distributions within the PCM. By analyzing different geometrical configurations, researchers can identify designs that mitigate the adverse effects of the air layer on the melting process.

Conclusions

The current study used ANSYS/FLUENT 16 software and numerical values to accomplish an analysis to examine the effect of an air layer on a material's phase transition. On PCM of paraffin wax, a quantitative study was performed (RT42). Several points have concluded in this work:

1. An increase in the air layer thickness has a quantifiable impact on the time needed to achieve the melting process. The analysis indicates a substantial increase in melting time as the air layer thickness grows, with a 125%, 136%, and 145% increase for air layer widths of 5 cm, 10 cm, and 15 cm, respectively.
2. The initiation of the melting process is consistently driven by the conduction load along the wall of the cell. This conduction-driven phase transition is marked by faster heat transfer at the beginning, gradually slowing down as the distance from the wall increases.
3. The role of natural convection becomes pronounced as the PCM moves away from the wall. This natural load-dependent heat transfer is observed to hinder the melting process, resulting in a gradual slowdown in the phase transition.
4. Cells without air layers exhibit faster heat transfer and shorter melting times compared to those with air layers.
5. The existence of an air layer above the cell is recognized as a noteworthy factor influencing the melting process. Thicker air layers impede heat transfer to a superior extent, extending the time necessary to complete the melting process.
6. The presence of an air layer above the cell was spotted to decline the PCM's ability to transfer heat efficiently. This decrease in heat transport is mirrored in the gradual slowdown of the melting process as the air layer thickness grows.
7. The dissolution process of the PCM is generally controlled by the existence of the air layer, with the side facing the air layer undergoing a relatively slower melting rate compared to the other sides.
8. The temperature at the top of the cell is meaningfully affected by the existence of an air layer. As the air layer thickness increases, a significant drop in temperature is detected. However, this effect lessens with additional increases in air layer thickness.

These results underscore the significance of considering environmental factors when designing PCM-filled cells for energy storage. Future analysis should optimize air layer thickness, study different PCM materials, and assess influences from ambient conditions. Additional simulations, especially dynamic or transient, experimental validation, and long-term stability estimations offer greater insights. Optimizing temperature gradients within the PCM and air layer is also critical for improving melting efficiency, minimizing energy losses, and refining the overall performance of PCM-based energy storage systems. By analyzing the thermal behavior of the PCM over multiple cycles, researchers can evaluate factors such as thermal degradation, phase change consistency, and energy storage capacity retention. Numerical simulations help predict the long-term performance of PCMs under cyclic loading conditions and inform strategies to maintain stability and efficiency over extended operational periods. Specifically, investigating multi-cell configurations, integrating with renewables, and advanced thermal management are crucial for real-world applications, enhancing efficiency and scalability in energy storage systems. One of the key limitations of the present research is the assumption of fixed thermo-physical parameters for PCM. This may not accurately simulate changes encountered in practice. Therefore, it would be prudent to observe how non-uniform material qualities influence the PCM while considering potential differences found in real-world settings.

Author contributions Conceptualization, A.F.K., F.L.R., M.A.A.-O., H.I.M., and A.A.; Methodology, A.F.K., F.L.R., M.A.A.-O., H.I.M., and A.A.; Software, A.F.K., F.L.R., M.A.A.-O. and H.I.M.; Formal analysis, A.F.K., F.L.R., M.A.A.-O., H.I.M., and A.A.; Investigation, A.F.K., F.L.R., M.A.A.-O. and H.I.M.; Resources, A.A.; Data curation, A.F.K., F.L.R., M.A.A.-O., H.I.M., and A.A.; Writing—original draft preparation, A.F.K., F.L.R., M.A.A.-O. and H.I.M.; Writing—review and editing, A.F.K., F.L.R. and A.A.; Visualization, A.F.K., F.L.R., M.A.A.-O., H.I.M., and A.A.; Project administration, F.L.R. and A.A. All authors have read and agreed to the published version of the manuscript.

Funding Open access funding provided by University of Gävle.

Data availability statement Data are contained within the article.

Declaration

Conflict of interest The authors declare no conflicts of interest.

References

1. Jawad, S.A., Redha, Z.A.A., Rashid, F.L.: Thermal performance of flat plate solar water collector using air bubble injection. AIP Conf. Proc. **2651**, 050019 (2023)
2. Rashid, F.L., Eisapour, M., Ibrahem, R.K., Talebizadehsardari, P., Hosseinzadeh, K., Abbas, M.H., Mohammed, H.I., Yvaz, A., Chen, Z.: Solidification enhancement of phase change materials using fins and nanoparticles in a triplex-tube thermal energy storage unit: Recent advances and development. Int. Commun. Heat Mass Transfer **147**, 106922 (2023)
3. Ali, H.M., Rehman, T., Arıcı, M., Said, Z., Duraković, B., Mohammed, H.I., Kumar, R., Rathod, M.K., Buyukdagli, O., Teggar, M.: Advances in thermal energy storage: fundamentals and applications. Prog. Energy Combust. Sci. **100**, 101109 (2024)
4. Ihnayyish, I.L., Ahmed, A.Q., Mohammad, A.T., Al-Syyab, A.K.S.: Numerical study to investigate the performance of U-shaped flat plate solar collector using phase change materials (PCMs). J. Tech. **5**, 74–80 (2023)
5. Khalaf, A.F., Rashid, F.L., Basem, A., Abbas, M.H.: Numerical study of the effect of air bubble location on the PCM melting process in a rectangular cavity. Math. Model. Eng. Probl. **10**, 71–83 (2023)
6. Hashim, A., Rashid, F.L., Abbas, M.H., Rabee, B.H.: Preparation of nanofluids from inorganic nanostructures doped peg: characteristics and energy storage applications. East Eur. J. Phys. **2023**, 185–188 (2023)
7. Rashid, F.L., Basem, A., Khalaf, F.A.A., Abbas, M.H., Hashim, A.: Recent breakthroughs and improvements in phase change material melting in a triple-tube thermal storage unit. Rev. Compos. Mater. Adv. **32**, 295–304 (2022)
8. De Gracia, A., Oró, E., Farid, M.M., Cabeza, L.F.: Thermal analysis of including phase change material in a domestic hot water cylinder. Appl. Therm. Eng. **31**, 3938–3945 (2011)
9. Mat, S., Al-Abidi, A.A., Sopian, K., Sulaiman, M.Y., Mohammad, A.T.: Enhance heat transfer for PCM melting in triplex tube with internal–external fins. Energy Convers. Manag. **74**, 223–236 (2013)
10. Shabgard, H., Bergman, T.L., Sharifi, N., Faghri, A.: High temperature latent heat thermal energy storage using heat pipes. Int. J. Heat Mass Transf. **53**, 2979–2988 (2010)
11. Tao, Y.B., Carey, V.P.: Effects of PCM thermophysical properties on thermal storage performance of a shell-and-tube latent heat storage unit. Appl. Energy **179**, 203–210 (2016)
12. Allouche, Y., Varga, S., Bouden, C., Oliveira, A.C.: Validation of a CFD model for the simulation of heat transfer in a tubes-in-tank PCM storage unit. Renew. Energy **89**, 371–379 (2016)
13. Hou, X., Gao, Y., Xing, Y., Xu, Z., Yin, J., Wang, S.: Bubble-injection and seeding enabled crystallization of erythritol/xylitol eutectic phase change material. Case Stud. Therm. Eng. **49**, 103278 (2023)
14. El Hasadi, Y.M.F.: Numerical simulation of the melting process of nanostructured based colloidal suspensions phase change materials including the effect of the transport of the particles. J. Mol. Liq. **287**, 110886 (2019)
15. Ebrahimi, A., Hosseini, M.J., Ranjbar, A.A., Rahimi, M., Bahrampoury, R.: Melting process investigation of phase change materials in a shell and tube heat exchanger enhanced with heat pipe. Renew. Energy **138**, 378–394 (2019)
16. Yan, Z., Yu, Z.J., Yang, T., Li, S., Zhang, G.: Impact of ultrasound on the melting process and heat transfer of phase change material. Energy Procedia **158**, 5014–5019 (2019)
17. Park, S.H., Park, Y.G., Ha, M.Y.: A numerical study on the effect of the number and arrangement of tubes on the melting performance of phase change material in a multi-tube latent thermal energy storage system. J. Energy Storage **32**, 101780 (2020)
18. Parida, A., Bhattacharya, A., Rath, P.: Effect of convection on melting characteristics of phase change material-metal foam composite thermal energy storage system. J. Energy Storage **32**, 101804 (2020)
19. Zeng, S., Chen, S., Wu, G.: Effect of inclination angle on melting process of phase change materials in a square cavity under mechanical vibration. J. Energy Storage **36**, 102392 (2021)
20. Chibani, A., Merouani, S., Benmoussa, F.: Computational analysis of the melting process of phase change material-metal foam-based latent thermal energy storage unit: the heat exchanger configuration. J. Energy Storage **42**, 103071 (2021)
21. Jaberi Kosroshahi, A., Hossainpour, S.: A numerical investigation on the finned storage rotation effect on the phase change material melting process of latent heat thermal energy storage system. J. Energy Storage **55**, 105461 (2022)
22. Li, C., Wais, A.M.H., Alizadeh, A., Mokhtari, M., Al-Azzawi, W.K., Abdul-sahib, N.Q., Shamsborhan, M., Lafta, H.A., Shams, M.A., Skikara, M., Hussien, B.M., Hekmatifar, M.: Melting process of RT-25 as a phase change material by placing innovative rectangular and parallelogram fins: effect of shape and angle of fins. J. Energy Storage **65**, 107375 (2023)
23. Tiji, M.E., Al-Azzawi, W.K., Mohammed, H.I., Dulaimi, A., Rashid, F.L., Mahdi, J.M., Majdi, H.S., Talebizadehsardari, P., Ali, H.M.: Thermal management of the melting process in a latent heat triplex tube storage system using different configurations of frustum tubes. J. Nanomater. **2022**, 7398110 (2022)
24. Ahmad, S., Ali, K., Ayub, A., Bashir, U., Rashid, F.L., Aryanfar, Y., Ali, M.R., Hendy, A.S., Shah, I., Ali, L.: Localized magnetic fields and their effects on heat transfer enhancement and vortices generation in tri-hybrid nanofluids: A novel investigation. Case Stud. Therm. Eng. **50**, 103408 (2023)
25. Ahmad, S., Ali, K., Sajid, T., Bashir, U., Lafta Rashid, F., Kumar, R., Ali, M.R., Hendy, A.S., Darvesh, A.: A novel vortex dynamics for micropolar fluid flow in a lid-driven cavity with magnetic field localization—a computational approach. Ain Shams Eng. J. **15**, 102448 (2024)
26. Rashid, F.L., Talib, S.M., Hussein, A.K.: An experimental investigation of double pipe heat exchanger performance and exergy analysis using air bubble injection technique. Jordan J. Mech. Ind. Eng. **16**, 195–204 (2022)
27. Mohammed, H.I.: Discharge improvement of a phase change material-air-based thermal energy storage unit for space heating applications using metal foams in the air sides. Heat Transfer **51**, 3830–3852 (2022)

28. Eisapour, A.H., Shafaghat, A.H., Mohammed, H.I., Eisapour, M., Talebizadehsardari, P., Brambilla, A., Fung, A.S.: A new design to enhance the conductive and convective heat transfer of latent heat thermal energy storage units. Appl. Therm. Eng. **215**, 118955 (2022)
29. Bais, A.R., Subhedar, D.G., Panchal, S.: Critical thickness of nano-enhanced RT-42 paraffin based battery thermal management system for electric vehicles: a numerical study. J. Energy Storage **52**, 104757 (2022)
30. Ghalambaz, M., Eisapour, A.H., Mohammed, H.I., Islam, M.S., Younis, O., Sardari, P.T., Yaïci, W.: Impact of tube bundle placement on the thermal charging of a latent heat storage unit. Energies (Basel) **14**, 1289 (2021)
31. Najim, F.T., Bahlekeh, A., Mohammed, H.I., Dulaimi, A., Abed, A.M., Ibrahem, R.K., Al-Qrimli, F.A., Mahmoud, M.Z., Awrejcewicz, J., Pawłowski, W.: Evaluation of melting mechanism and natural convection effect in a triplex tube heat storage system with a novel fin arrangement. Sustainability **14**, 10982 (2022)
32. Eisapour, M., Eisapour, A.H., Shafaghat, A.H., Mohammed, H.I., Talebizadehsardari, P., Chen, Z.: Solidification of a nano-enhanced phase change material (NePCM) in a double elliptical latent heat storage unit with wavy inner tubes. Sol. Energy **241**, 39–53 (2022)
33. Longeon, M., Soupart, A., Fourmigué, J.F., Bruch, A., Marty, P.: Experimental and numerical study of annular PCM storage in the presence of natural convection. Appl. Energy **112**, 175–184 (2013)